ESCOLA POLITÉCNICA DA UNIVERSIDADE DE SÃO PAULO
LUIZA DE LIMA SODERO

Compaction, sintering and characterizations of nanometer-sized alumina: effects of surface state of nanoparticles

São Paulo
2021

LUIZA DE LIMA SODERO

Compaction, sintering and characterizations of nanometer-sized alumina: effects of surface state of nanoparticles

Trabalho apresentado à Escola Politécnica da Universidade de São Paulo como atividade obrigatória da disciplina PMT-3596

Área de Concentração:
Engenharia de Materiais

Professor:
Prof. Dr. Douglas Gouvea
Prof. Dr. Lucile Joly-Pottuz
Prof. Dr. Vincent Garnier
Prof. Dr. Joel Lachambre

São Paulo
2021

ACKNOWLEDGEMENTS

This paper comes from a distinct semester of study and research as a part of the Ceramic Team (CERA) from MATEIS (Matériaux Ingénierie et Science) as a PFE intern and I could not bring an end to this journey without acknowledging the people around me along this period.

The only fair way to start this section is thanking the SGM department for accepting my candidature nearly 2 years ago to become a Double Degree student. Also, I would like to specially thank M. Jarir Mafound and Ms. Haridian Melgar for all their support from the beginning to the very end. All of us, Brazilian students you selected, are forever grateful for this opportunity.

Thank you to all three of my tutors, Ms. Lucile Jolly-Pottuz, M. Vicent Garnier and M. Joel Lachambre, for giving me the chance to be a part of your studies as well as for always being available for any of my questions, and especially for your patience. And a special thank you to my Brazilian tutor, Douglas Gouvea, for the support given from such a big distance.

For the students that were part of my academic life, in Brazil and especially in France, I would not just say thank you, I would include my best wishes for your upcoming careers. I would also love to thank the professors that were indirectly part of this research, Ms. Sandrine Cardinal for the formation on the XRD; M. Laurent Gremillard for also giving me support on the XRD specters; M. Jules Galipaud for the XPS measurements and for Sylvie Le Floch for the support given from the Lyon 1 laboratory. Finally, I need to thank my family for all the support given to me even if we are separated by an ocean. They have always been the ones to encourage my wildest dreams as well as to give me all the bases I needed to go through with them. For teaching me to always value education the most, thank you from all my heart.

ABSTRACT

This research paper on transition alumina aims to comprehend the comportment of compacted thin samples. Multiple characterizations methods were used to determine whether the surface state impacts in compaction and how it could improve sintering. The starting powder is provided by NanoTek®, and it is a transition alumina. From this powder, other two were elaborated to create opposite conditions and to discover whether this would change the final material. The dry powder is kept at 900°C for 10 hours and the humid one is stocked in a confined and humid atmosphere at 25°C for 3 days. From these powders other samples were elaborated by compaction, at 5GPa and 15GPa, and some were also sintered at 900°C. The characterization of these samples was done by X-Ray Diffraction (XRD) and Spectroscopy (XPS) as well as Infrared spectroscopy (FTIR). Finally, the image taken from an in-situ nano compression test of a Scanning Transmission Electron Microscope (STEM) was studied to evaluate the pertinence of implementing Digital Imaging Correlation in the image processing. Nano compression proved there is a great difference in behavior between the two compacted samples, because the thin layer obtained from the humid sample did not stand the indentation because of a lack of consistency between particles at this level. And the XRD analysis showed the humid powder generates a greater percentage of diaspore.
Keywords: Alumina, Characterization. Phase Transformation.

SUMÁRIO

OBJECTIVES

There are three main objectives on this paper on transition alumina. Firstly, achieve better understanding how compacted thin samples behave through four methods of characterization. Secondly, determine whether the initial superficial state of the alumina powder impacts on the final compacted and/or sintered samples. Lastly, evaluate the pertinence of Digital Image Correlation on in-situ mechanical tests on micrometric samples of alumina.

1 INTRODUCTION

This section will present the bibliographical research done on alumina and its transitions phases, as well as its behavior during deformation; and also on Digital Image Correlation (DIC) as a method to quantify the displacement of particles in alumina.

1.1 NANOCERAMICS AND ALUMINA

The development of nanomaterials lies on the interest to improve performances on many industries – like medical, chemical, electronic, environment - because the physical properties of a material can change considerably when it goes from the conventional scale to the nanoscale. A better understanding of the characteristics of nanomaterials could allow the enhancement of mechanical properties that may bring innovations on many sectors1. Nanoparticles have a bigger atom fraction in the grain boundaries which means they have a more important surface energy.

Nanoceramics are a special kind of material because it requires the mastering of elaborations processes, shaping, sintering, machining and characterizations, because they play a big role on the obtained microstructure in function of the desirable final properties.

Even though ceramics are known to be brittle materials, recent studies have shown that plasticity is possible on these materials at low temperature2. Phase transformation may also occur under pressure even at ambient temperature3.

Alumina is the aluminum oxide known as Al2O3. It is the second hardest material, only losing to diamond, has a good biocompatibility, is a low heat conductor and is a great electrical insulator. The interest in understanding better ways to elaborate and process alumina is linked to the many possibilities it could bring.

This oxide can be obtained industrially from bauxite through the Bayer process4, and can be purified to metallic aluminum with the Heroult-Hall process5. But to obtain

[1] AZAR, Mirella, Mise en forme et frittage des poudres de céramique nanostructurées : « Cas d'une alumine de transition », p. 146, .
[2] CALVIÉ, Emilie *et al*, Real time TEM observation of alumina ceramic nano-particles during compression, **Journal of the European Ceramic Society**, v. 32, n. 10, p. 2067–2071, 2012.
[3] ISSA, I. *et al*, Room temperature plasticity and phase transformation of nanometer-sized transition alumina nanoparticles under pressure, **Acta Materialia**, v. 150, p. 308–316, 2018.

ultrafine nanoparticles, the method used the most is the PVS (Physical Vapor Synthesis) or Inert Gas Condensation, a schema is shown in Fig. 1. It consists of evaporating the material inside a chamber that is evacuated to a vacuum and then backfilled with a low-pressure inert gas.

Figure 1 — Schema for the Physical Vapor Synthesis of nanopowders

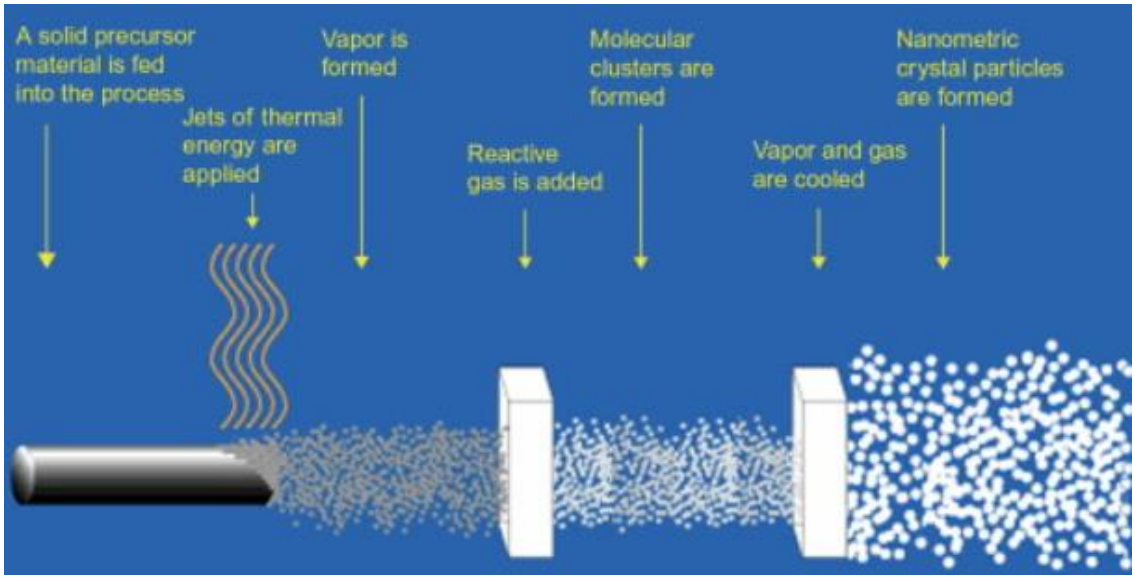

Source: **Laser Ablation - an overview | ScienceDirect Topics**, available: <https://www.sciencedirect.com/topics/physics-and-astronomy/laser-ablation>. Accessed on: 2 mar. 2021.

1.1.1 Phases of alumina

Alumina can be found in different crystallographic phases. The most common one is alfa alumina, which can also be called corundum, that is stable at bulk; its oxygen anions are arranged in hexagonal compact form (HCP, Fig. 2a) with the aluminum cations filling 2/3 of the octahedral sites, and 1/3 of these vacancies are ordered along a rhombohedral structure axis[6].

Transition alumina on the other hand is only stable at nanoscale. The known phases are gamma(γ), delta(δ), eta(η), chi (χ) and theta(θ). The oxygen anions are arranged in a Face Centered cubic arrangement (FCC, Fig. 2b). The aluminum cations occupy both tetra and octahedral sites, and each phase has a specific percentage of those

[4] ROUZAUD, Djibril, Essais de Nanocompression In Situ en STEM d'une Alumine Compactée : Développement du traitement d'images pour suivre le déplacement des nanoparticules, p. 14, .
[5] **Alumínio: Ocorrência, obtenção industrial, propriedades e utilização**, disponível em: <https://educacao.uol.com.br/disciplinas/quimica/aluminio-ocorrencia-obtencao-industrial-propriedades-e-utilizacao.htm>. acesso em: 24 fev. 2021.
[6] ISSA *et al*, Room temperature plasticity and phase transformation of nanometer-sized transition alumina nanoparticles under pressure.

cations occupying octahedral sites instead of tetrahedral ones. The arrangement of cations in the gamma phase is cubic and, in the delta, one is tetrahedral, while in delta star(δ*) it is orthorhombic[7].

Figure 2 - Crystallography of the different alumina phases (a) HCP and (b)FCC

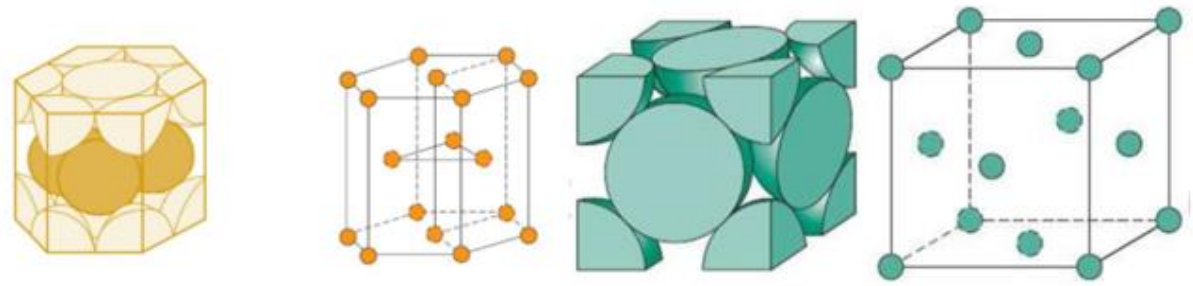

Source: PERSECHINO, Italo, Development of a polycrystal plasticity simulation tool including recrystallization (DRX) phenomena, 2017.

The transformation is irreversible and is usually observed as Boehmite(γ-AlOOH)→Gamma(γ-Al2O3)→Delta(δ-Al2O3)→Theta(θ-Al2O3)→Alfa(α-Al2O3)[8]. A way to identify which phase is present in a sample is to pass it through an X-Ray Diffractometer and identify its peaks using their JCPDS file (Joint Committee on Powder Diffraction Standards)[9]. For this study, four files were used, γ (00-050-0741), δ (00-016-0394), δ*(00-046-1215) and α (00-046-1212).

Another important structure in the phase transformation of alumina is Diaspore, a structure that reveals that the transformation to alfa alumina went through a direct transition instead of going step by step on the previously mentioned oxides.

1.2 IN-SITU MECHANICAL IN TRANSMISSION ELECTRON MICROSCOPE

From the need to closely observe the movement of dislocations in a material during a mechanical test, a method to record it inside a Transmission Electron Microscope (TEM) was proposed by IMURA, T in 1974.[10] Nowadays there are multiples approaches for this kind of measurements as shown by LEGROS, M in 2014[11], in

[7] *Ibid*.
[8] *Ibid*.
[9] ICDD Database Search – ICDD.
[10] IMURA, T. *et al*, In-situ dynamic observation of dislocation motion at low and high temperatures by HVEM, **The Proceedings of the Third International Conference on High Voltage Electron Microscopy**, p. 199–205, 1974.
[11] LEGROS, Marc, In situ mechanical TEM: Seeing and measuring under stress with electrons, **Comptes Rendus Physique**, v. 15, n. 2–3, p. 224–240, 2014.

which new equipment is implemented inside a Transmission Electron Microscope to extend the efficiency and capabilities of in situ deformation studies.

Fig. 3 shows the equipment for a uniaxial tensile test, which is not so different from a conventional test apart from the size, so the expertise that is important in this test is creating micro sized gear to be installed inside the microscope. Although the image retrieved itself is still quite underexploited, A way to analyze these images is given by the DIC method which has been gaining space in the field. Nowadays the challenge is joining data analysis methods and storage to the multiple cameras implemented to capture the dynamical test.

1.2.1 Digital Image Correlation (DIC)

Digital Image Correlation (DIC) is a method to measure the displacement or deformation camp from images taken during an in-situ mechanical test. The principle consists of comparing two images, the reference and the deformed one, and determining the displacement from one to the other. The calculation of this displacement generates a residue, that measures the quality of the correlation, and in each calculation the aim is to minimize this value. The quality of this computing relies on the variations of luminosity or contrast between the images as well as the noise from the machine. Fig. 4 shows an example of the treated image to be used in the DIC.

To obtain the points of the calculation a mesh must be done on the free surface as to extract an envelope for the sample. The nodes having the same gray scale as air are automatically erased for the calculation as to only analyze the important surface. The meshing is also more refined closer to the indent as to have better results, meanwhile the mesh farther from this point is more spaced to guarantee a faster calculation. An important point here is that this mesh must respect the morphology of the fissure. An exploitation of the correlation residue is needed to find the surface of the fissure since cavities and the fissure itself belong in the residue, so that is where the morphology and the localization of the fissure data is kept.

Figure 3 - a) Schematic stress–strain curve for a uniaxial tensile test performed on a macroscopic dog-bone shaped specimen (insert). Point 3 corresponds to the transition between elastic (gray) and plastic (pink) regimes of the curve. The corresponding stress is called the yield stress or σy . b) Samples for in situ TEM straining. Rectangular shaped sample glued on a copper grid (upper right) or directly shaped as a dog bone (lower right). Note the dimple at the center of both samples, where e-

transparency is achieved. c–d) Standard straining holders based on electric motor and worm gear actuation. c) Principle, d) commercial room temperature holder for FEI microscope made by Gatan

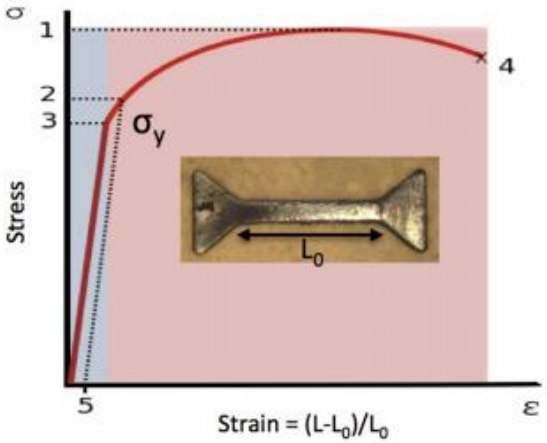

a)

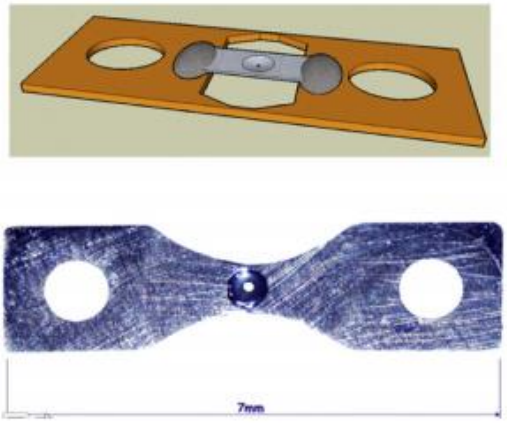

b)

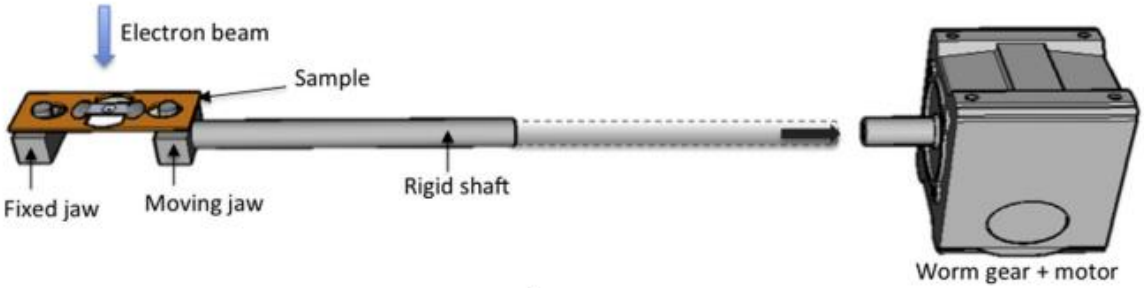

c)

d)

Source:

Figure 4 – Example of Image Processing

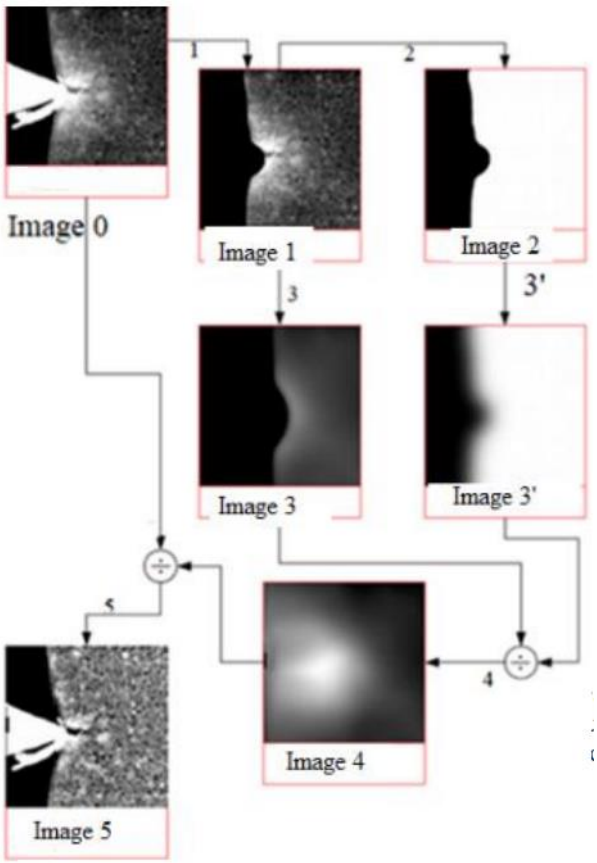

Source:

2 MATERIALS AND METHODS

The starting powder for the experimental part of this research was provided by NanoTek®, Nanophase Technologies Corporation located at Romeoville, IL, USA). It is a transition alumina obtained from Physical Vapor Synthesis (PVS).

2.1 PREPARATION

From the supplier, two new powders will be elaborated, one should be the driest possible – and will be called dry powder (DP); and the other will be maintained in humid atmospheres – also called humid powder (HP).
The process of drying consists of placing a portion in an oven that was heated at a rate of 2°C/min until reaching 900°C; it is kept at this temperature for 10 hours and lastly, the oven is cooled at the same rate until 100°C. It is finally conserved in a small container well closed inside a desiccator.
To hydrate the powder, a portion is stocked in a confined and humid atmosphere at 25°C for three days.

2.1.1 Compression and sintering

The following manipulations were done in collaboration with the ILM (Institut Luminère Matière), a research laboratory of the CNRS (Centre National de la Recherche Scientifique) and Lyon 1 (Claude Bernard Université). From both powders, different samples were compressed and/or sintered with different methods. Firstly, each of the powders is compacted by hand using a piston inside a gold capsule, to avoid contamination. Their heights are measured, the cylindric samples obtained from the dry powder was 0.51mm and from the humid as 0.93mm of height. From those samples, thin blades were made using Focus Ion Beam (FIB) to go through in situ nano compression inside a TEM. This samples are referenced as GDP and GHP, respectively for the compacted samples form the dry and the humid powder.
Afterwards, a sintering under pressure was done on those samples, consisting of compression and decompression at rate 0.1GPa/min until 5GPa and heating at 100°C/min until 560°C. It is then kept in this level for 15 minutes and then it is dipped in water to cool down to room temperature. This samples will be referenced as SCD-1 from the dry powder and SCH-

Two other compacted and sintered samples were done from the dry powder for comparison. One was made using an iron pellet and the other was compressed using glycerol in the pellet at 700 MPa, their reference is respectively SCD-I and SCD-G. Both unmoldings showed that since the powder is quite abrasive, there is some material that gets stuck in the mold.

Another compaction was done under 15GPa in Boron-epoxy gasket in a Paris Edinburgh Press[12], figure 5 shows the gasket in question. The dry powder compressed resulted in a cylindric sample with diameter of 800µm and 1.7mm of height, HPD. The humid powder had 1mm of diameter, HPH.

Figure 5 - Paris Edinburgh Press Gasket

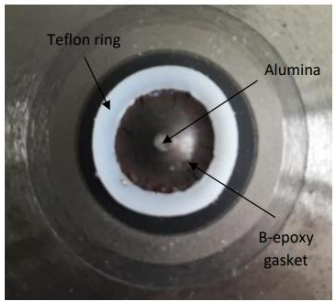

Source: Author's own

To summarize all samples to be characterized, Table 1 shows all nine of them.

Table 1 – Acronyms used for each sample

	Reference	Sample
1.	DP	Dry Powder
2.	HP	Humid Powder
3.	GDP	Gold Capsule Hand Compacted from DP
4.	GHP	Gold Capsule Hand Compacted from HP
5.	SCD-1	Sintered and Compacted from DP
6.	SCD-I	Iron pallet sintered and compacted from DP
7.	SCH-G	Glycerol pallet sintered and compacted from DP
8	SCH	Sintered and Compacted from HP
9.	HPD	15GPa-Compacted from DP
10.	HPH	15GPa-Compacted from DP

[12] LE FLOCH, Sylvie, **Presse Paris-Edinburgh**, PLECE, disponível em: <http://plece.univ-lyon1.fr/index.php/uipements-mainmenu-38/paris-edimbourg>. acesso em: 25 fev. 2021.

2.2 CHARACTERIZATION

Each method of characterization had a type of sample, although some of them were able to measure both the compressed ones and the powders.

2.2.1 X-Ray Diffraction

The machine used for this analysis was a Bruker D8 using Cu-Kα radiation (λ=0.154nm) and the measurement was set up using its software XRD Wizard that creates a parameter file. The important parameters to be set were the two-theta angle, from 10 or 20° to 80°, using 0.02° for each step for 16 seconds. This file is implemented using the measuring software, XRD Commander, by creating a job that lasts 17 hours.

In total, eight samples underwent X-Ray Diffraction, both powders (DP and HP), both high pressure compacted samples (HPD and HPH) and four samples compacted at 5GPa (SCD-1 and 2 and SCH-1 and 2). The reason behind these many sintered samples is that they were each sintered differently because the first compacted sample of the dry powder made in the gold capsule resulted in a dark disk that suggested a contamination of the sample, even though this should be quite unlikely in this type of capsule. So, other two were prepared differently, firstly one was made using an iron pellet that did not contaminate the sample but also resulted in a dark-like sample, although usually alumina is lighter colored and even transparent at times. Finally, the sample made using glycerol had different aspects, the top side had the expected appearance but the other one had black stains, probably from the pellet – because of this, both sides were analyzed.

2.2.1.1 Peak Identification

The identification of peaks is done using the analysis software, EVA, by also knowing the JCPDS files of the expected alumina and considering possible contaminants, like iron, gold and carbon.

2.2.1.2 Refinement

Initially the refinement done was expected to be Rietveld using the TOPAS software, but because the peaks of each transition alumina are quite close, it becomes too

hard to make a truthful analysis. Despite this, a refinement by *hkl* phase was done, which consisted of filling the desired crystallography in the software by hand instead of loading their CIF files from the COD database (Crystallography Open Database)[13], this measurement is more of a estimative since the user is in control of which parameters the software uses in its calculation. The Rietveld method could be used for the sintered samples because the peaks were more distinguishable for alfa alumina and diaspore.

The spectrograms from both powders and their compressed and sintered cylindric samples underwent this process. The compressed samples could not be refined by this method because their peaks gave an untruthful measurement.

2.2.2 X-Ray Photoelectron Spectroscopy

In collaboration with the Laboratory of Tribology and Dynamic of Systems (Ecole Centrale de Lyon), three compacted cylindric samples from the Paris-Edinburg Press underwent X-Ray Photoelectron Spectroscopy, two from the humid powder and the other from the dry one. They were fixed in the sample holder with a scotch tape that could potentially contaminate the sample with carbon. Their mass was also measured to evaluate whether the depressurizing of the chamber could have an impact on the sample. Their masses were measured before and after the measurement, since the depressurization of the chamber is supposed to remove adsorbed water from the sample.

The microscope was the XPS Versaprobe II de la marque ULVAC-PHI using Al K alpha monochromatized at 1486.6 eV as source. The angle between the source and the analyzer was 45°. The measurement was done under vacuum at $2*10^{-9}$ using transient energy of 187 eV during the overview of samples and 23 eV when obtaining high resolution specters. The diameter of the measuring zone was 50μm. For the quantification, les factors de sensibility used were proposed by WAGNER, CD[14] correcting its value according to the machine's transmission and its angular distribution.

---

[13] **Crystallography Open Database**, disponível em: <http://www.crystallography.net/cod/>. acesso em: 24 fev. 2021.

[14] WAGNER, C. D. *et al*, Empirical atomic sensitivity factors for quantitative analysis by electron spectroscopy for chemical analysis, **Surface and Interface Analysis**, v. 3, n. 5, p. 211–225, 1981.

Fig. 6 is a photograph taken before inserting the samples inside the XPS chamber. Each sample had three points to be measured, avoiding possible impurities, and choosing two points at the center and one closer to the edge. Two methods of measurement are done, firstly the Sureval, which corresponds to a specter obtained faster just to determine if the positioning and parameters are correct for each point; and then the longer measure is done with high resolution, this one reveals the chemical state of the elements as well as its bonds.

Figure 6 – Position of samples at the XPS

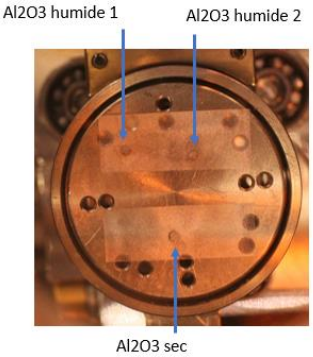

Source: Author's own

2.2.3 Infrared Spectroscopy

Infrared Spectroscopy was carried out by ThermoFischer scientific Nicolet iS50 equipment. Two different manipulations were done in infrared, using the samples as they already were and another after dissolving the powder in a solution of KBr. For this last one, to elaborate the solution, the KBr powder was left in an incubator at 110°C overnight. The nano powder is diluted at 1% in mass in KBr of >99.5% purity and placed in a pelletizer of 13mm. The obtained data was processed using Microsoft's Excel.

2.2.4 In situ nano compression in the STEM

A nano-compression test was performed inside a Scanning Transmission Electron Microscope (STEM) with a High Angle Annular Dark Field detector (HAADF) to obtain the image of a thin film being deformed. Two samples were supposed to be indented, the compacted samples at 15GPa from both powders. The obtained film was processed using ImageJ-Fiji developed by US National Institutes of Health. The

important points to master in the processing is eliminate the noise and highlight the constitutive particles around the deformation area. The DIC method is implemented on a series of images taken in regular intervals de temps to determine the displacement of the nanoparticles.

3 RESULTS

3.1 DIASPORE FORMATION

To measure the quantity of diaspore possibly formed in the humid powder, a portion of it is weighed ($m_O = 1.006g$) and kept in an incubator for 4 days at 100°C. The mass is measured again ($m_F = 0.936$) to quantify the loss of water ($m_{H20} = 0.070g$), which means $n_{H20} = 3.889 * 10^{-3}$mol of water was lost could be part of the formation of diaspore. From the final alumina mass, and since it is not a hydrated compound, 9.176*10^{-3} mol of alumina was maintained. In fact, the molar fraction of water was around 0.3 and of alumina was 0.7. Diaspore is obtained as shown in Eq. 1

$$Al_3O_2 + H_2O \rightarrow 2\,AlO(OH) \quad (1)$$

If all the lost mass were in this reaction as water, the diaspore produced would be $n_d = 7.78 * 10^{-3}mol$ or $m_d = 0.467g$. Overall, half of the initial alumina could have turned into diaspore. It could also be interesting to measure the mass of the powder before hydration to make this estimative.

3.2 COMPACTION AND SINTERING

After compaction by hand in the gold capsule of each powder, knowing the displacement of the piston, the change in volume can be calculated, and therefore, the compaction. A mass of 58 mg of the dry powder was initially compacted at 22% and a mass of 88 mg of the humid powder was compacted at 33%. The second sample done from the dry powder, with 60mg, had 23%. Overall, the humidified powder compress more easily than the dry one.

When removing samples from the compaction capsule, they have a tendance to delaminate. For example, after compaction and sintering of the humid powder, three disks were taken with a translucid-like appearance and some black spots that are probably due to contamination during manipulation. Fig. 7 shows images taken from the binocular microscope from the laboratory.

Figure 7 - Images taken with the binocular microscope of the humid Powder after compaction and sintering

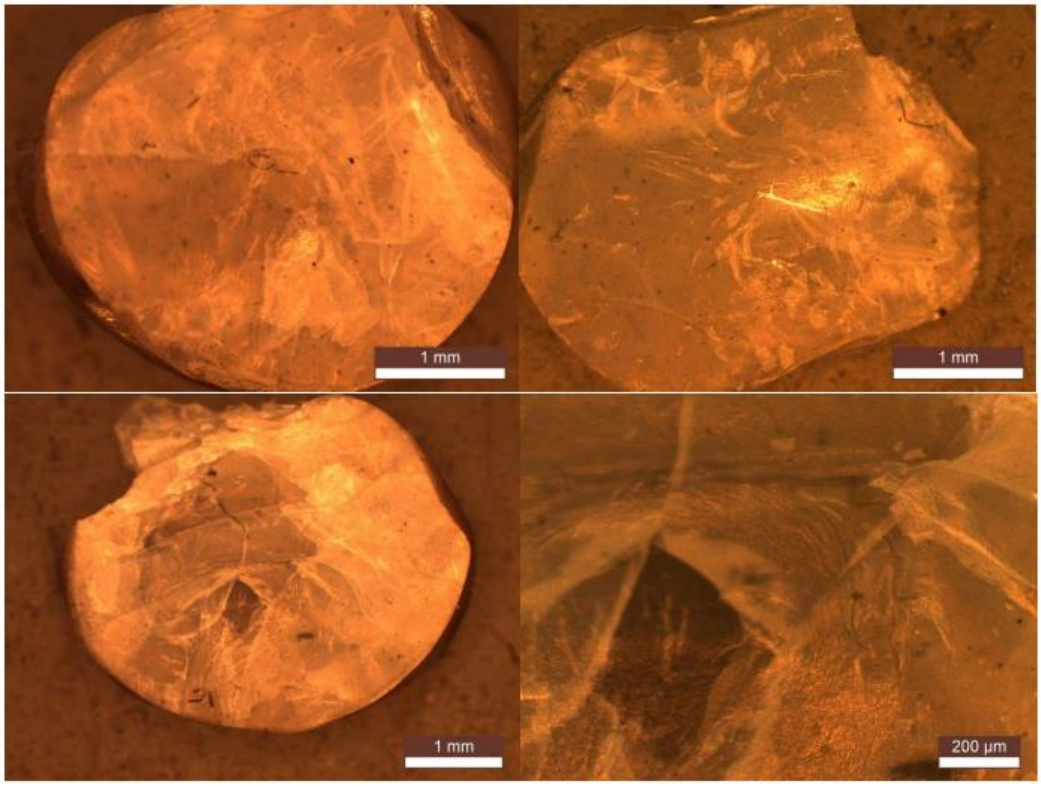

Source: Author's Own

The sintering of the second sample done with the dry powder resulted in a much smaller volume but without a true cylinder format; the only way to remove the sample was in small transparent pieces with a few micrometers, Fig 8 shows two micrographs taken from the particles taken from this manipulation.

Figure 8 - Images taken with the binocular microscope of the dry powder after compaction and sintering

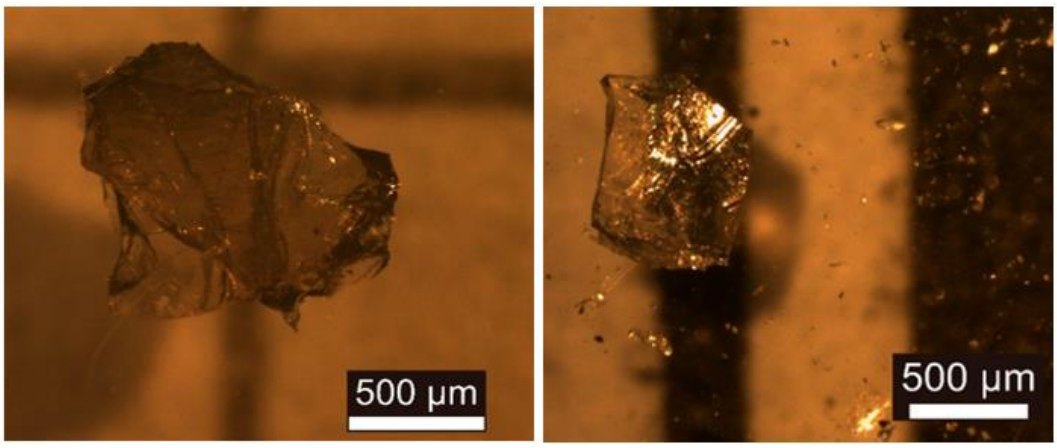

Source: Author's own

Fig. 9 shows the appearance of the sample from the dry powder after compaction at 15GPa using the Paris-Edinburgh Press. At the middle of the sample, it is possible to see a fissure that proves the higher pressure at the center of the gasket. Figure 10 shows the sample from the humid powder.

Figure 9 – Image taken with the binocular microscope of the dry and compacted sample removed from the Paris Edinburgh Press

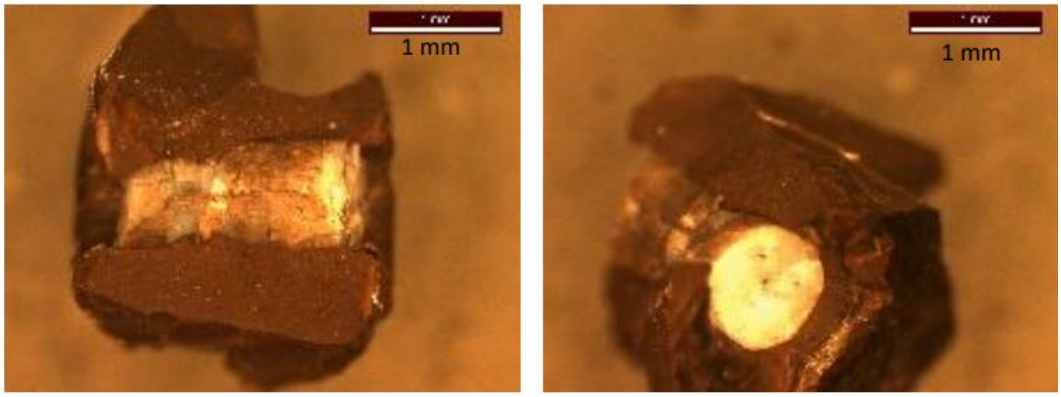

Source: Author's own

Figure 10 - Image taken with the binocular microscope of the dry and compacted sample removed from the Paris Edinburgh Press

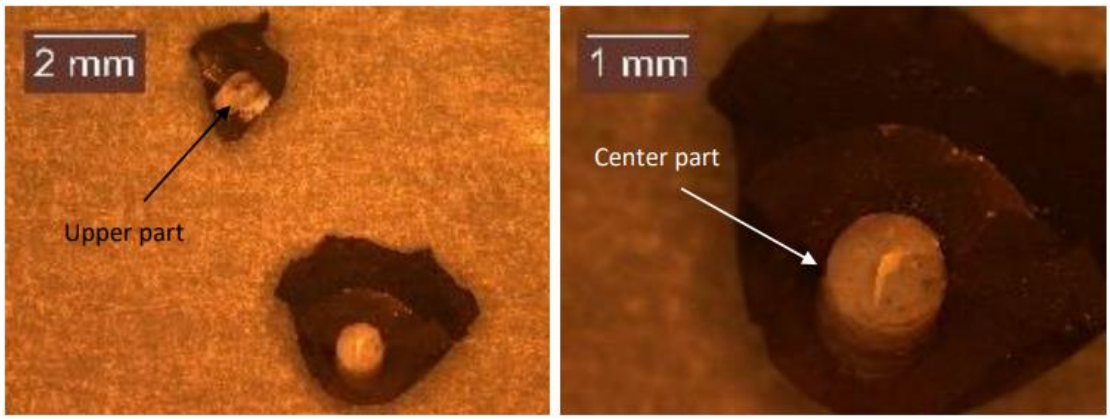

Source: Author's own

3.2.1 FTIR of compressed samples

Fig. 11 shows the obtained specter from the FTIR analysis of both starting powders and their state after compaction. The broad peak around 3500cm-1 corresponds to a free linked OH[15] and it is only present in the humidified powder.

[15] **Table Infra-rouge : interprétation des spectres IR**, disponível em: <https://www.lachimie.fr/analytique/infrarouge/table-infra-rouge.php>. acesso em: 10 fev. 2021.

Usually, a peak between 3500-3700 is linked to OH in a free bond, which could be the ion adsorbed on the surface, Meanwhile, when the peak is at 3100-3500 it represents the OH bonded by hydrogen bridges, which could possibly attest the presence of aluminum hydroxide. Another evidence of water in this specter is the well-defined peak at 1640 corresponding to water[16]. This demonstrates that compaction eliminates a great part of the water present. The presence of water is the only difference between the starting powders.

Figure 11 – FTIR obtained on both starting powders before and after compaction

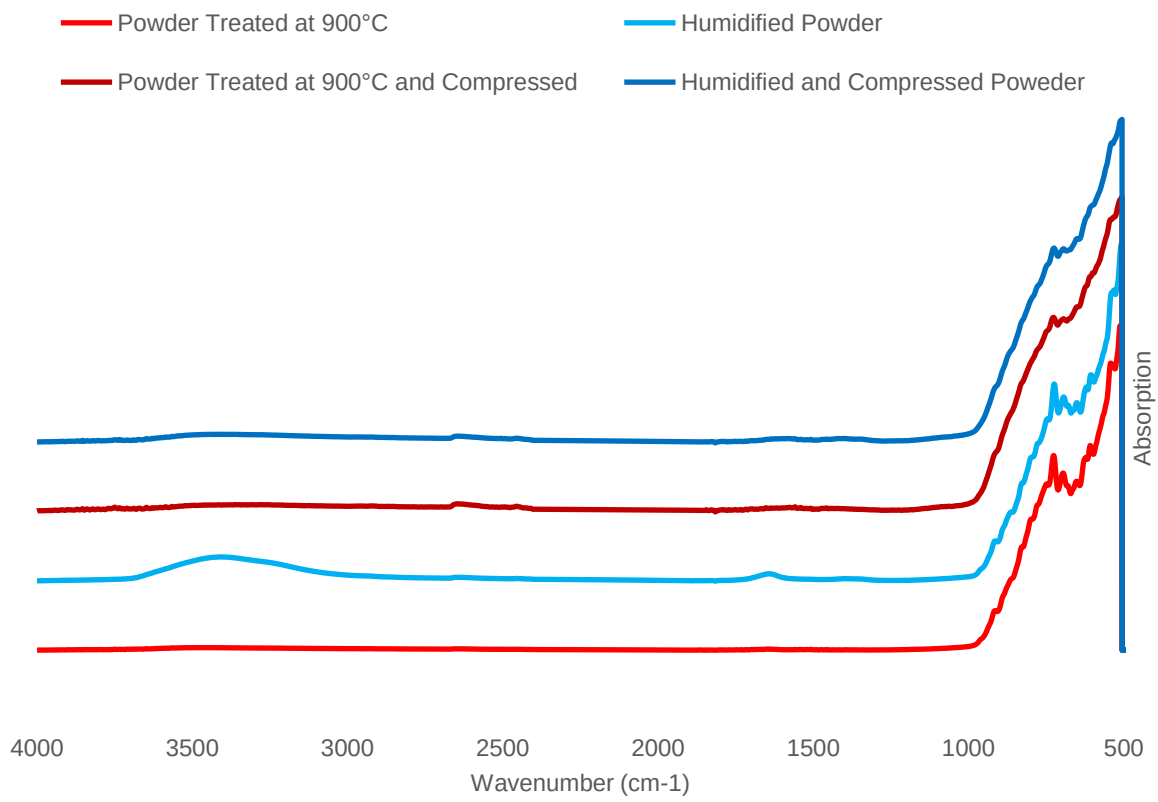

Source: Author's own

For both powders, after compaction, the peaks become smother, and the 500-1000cm-1, in Fig. 12, reveals the peak that corresponds to carbonate around 700[17] for all samples, which is also the one used to normalize the curves. The presence of adsorbed carbonates in the sample could be linked to the atmosphere of the

[16] **Molecular Vibrations Explained | Animated Guides - Specac**, disponível em: <https://www.specac.com/en/news/calendar/2019/03/molecular-vibrations>. acesso em: 27 fev. 2021.

[17] MAGLIONE, Gilbert; CARN, Michel, Spectres infrarouges des minéraux salins et des silicates néoformés dans le bassin tchadien, p. 7, .

manipulation even though the dry powder was safely kept in a glovebox. The absorption is higher starting at 1100cm-1 is related to the occupancy of the tetrahedral sites by Al+3 in the FCC lattice, which corresponds to transition alumina[18]. As shown by TARTE, tetrahedrally coordinated aluminum oxide compounds absorb highly in this region[19]. Annex A shows the brute specters for reference with the OH bands, CO3, H2O and Al+3 peaks identified.

Figure 12 - FTIR of the four samples in the 500-1000 region

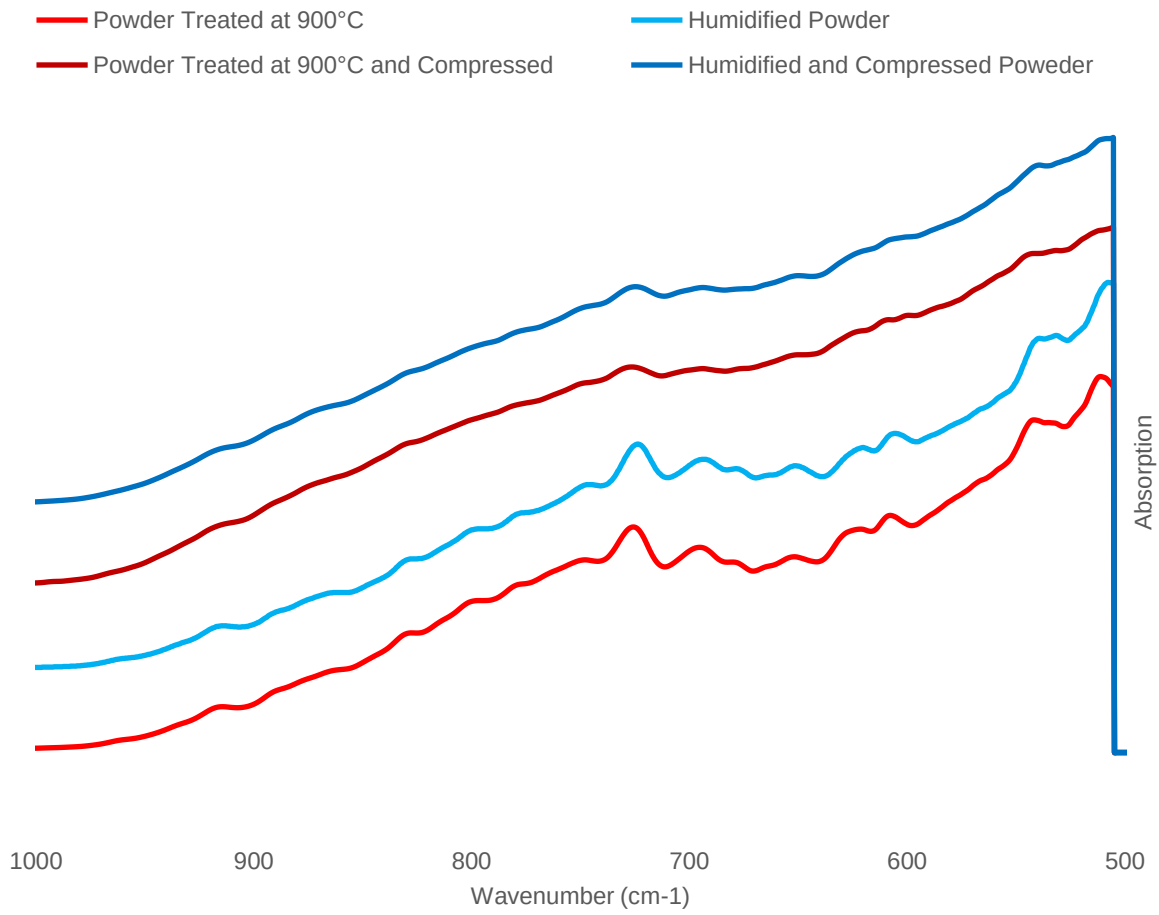

Source: Author's own

The FTIR measurement done for the powders diluted in 1%wt of KBr are shown in figures 13 to 16 as graphs of Transmission as a function of the wavelength. In Fig. 13, the humid powder has three peaks that are linked to adsorbed water – 1384,1636

[18] BUSCA, Guido *et al*, Surface sites on spinel-type and corundum-type metal oxide powders, p. 8, .

[19] TARTE, P., Infra-red spectra of inorganic aluminates and characteristic vibrational frequencies of AlO4 tetrahedra and AlO6 octahedra, **Spectrochimica Acta Part A: Molecular Spectroscopy**, v. 23, n. 7, p. 2127–2143, 1967.

and 3475. It is important to know that the KBr solution is quite hydrophilic and could make these peaks more prominent than it is, as seen in the previous analysis. The presence of a peak linked to carbon is also present like before.

Figure 13 – : FTIR of the humid powder in solution

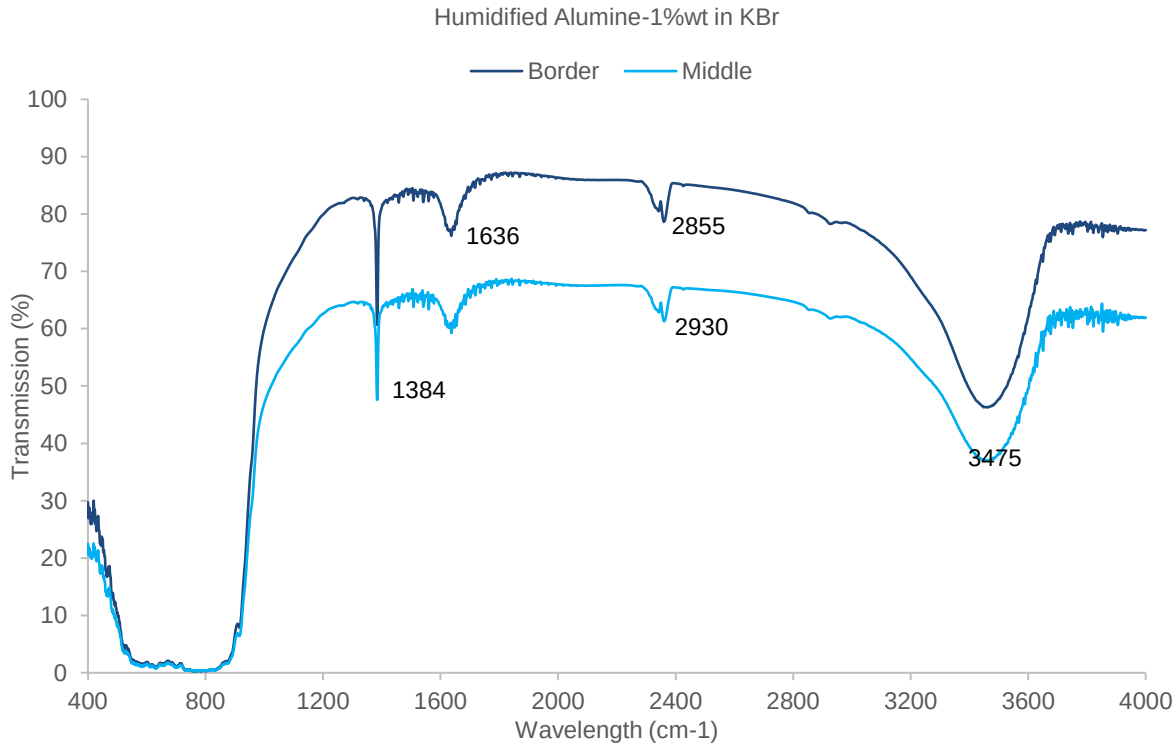

Source: Author's own

In Fig. 14, the dry powder does not have such prominent peaks for water, but they are present, which could be caused by the KBr solution. In Fig. 15, the starting powder, without any treatment, is shown with expressive peaks related to water (1620) and OH (3400) bonds as well as carbon (2356).

Figure 14 – FTIR of the dry powder in solution

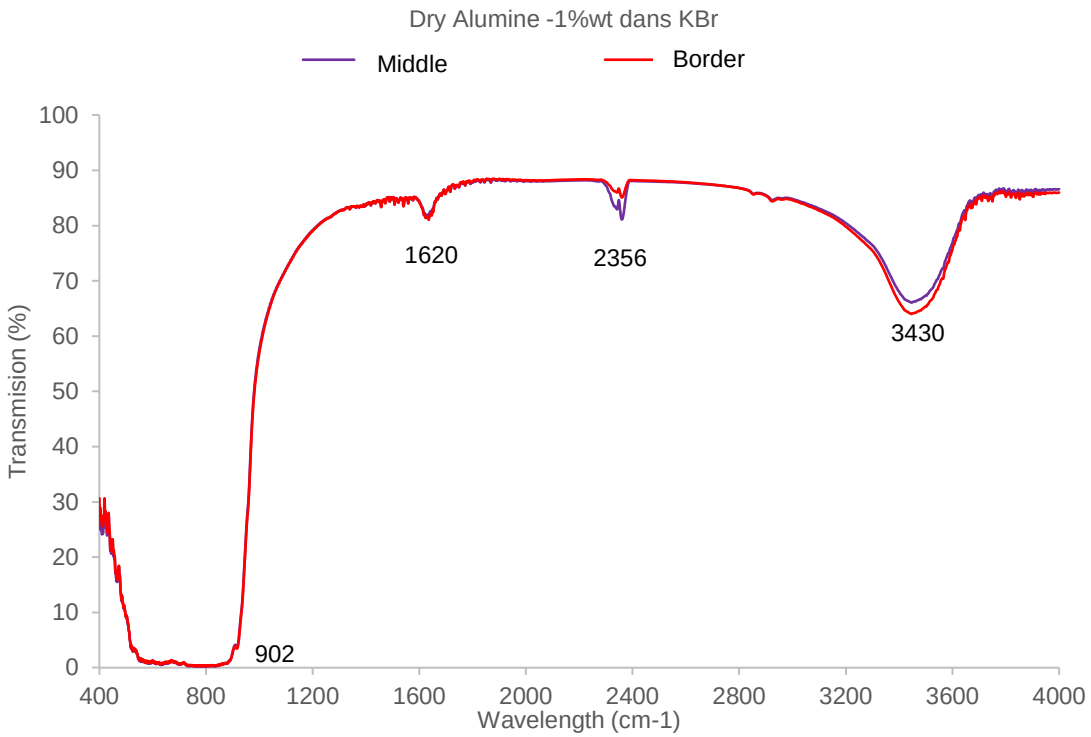

Source: Author's own

Figure 15 – FTIR of the starting powder

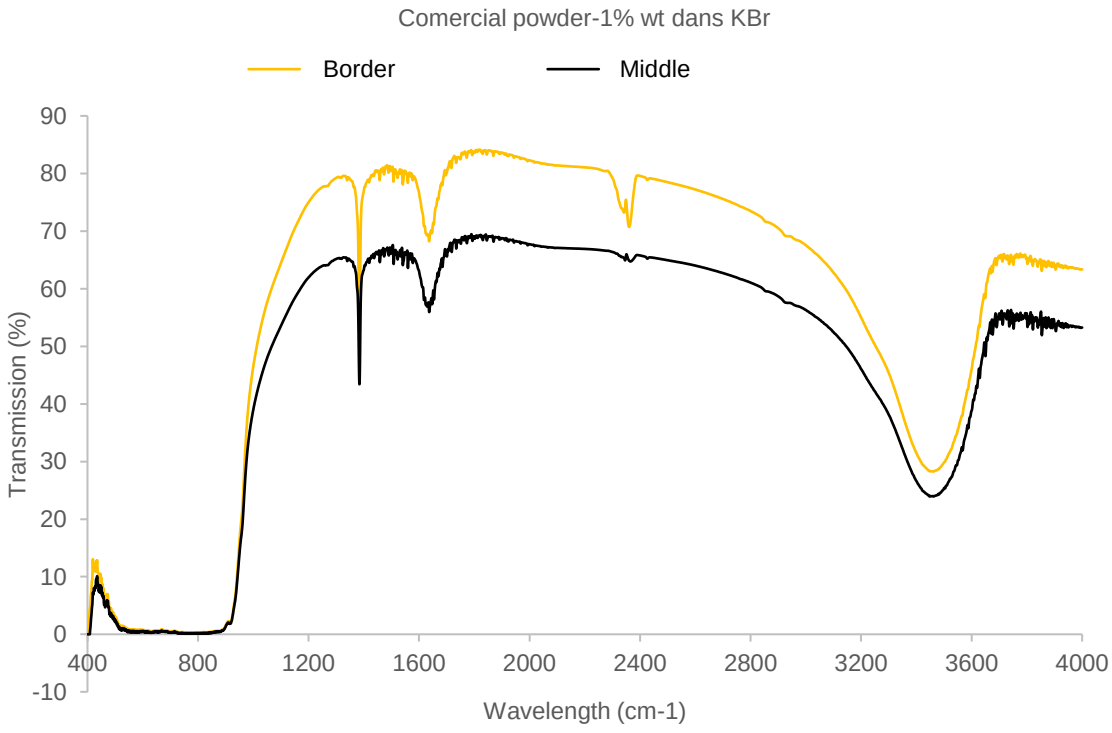

Source: Author's own

For reference, a measure of the pastille was done with only KBr in open air (Figure 16), and the peaks for carbon (1380) and OH (3400) are present (Figure X+3). There is a possibility that the presence of carbon is just a common contamination linked to the atmosphere. Carbonates are found frequently in nano powders of oxides.

Figure 16 – FTIR of the KBr powder

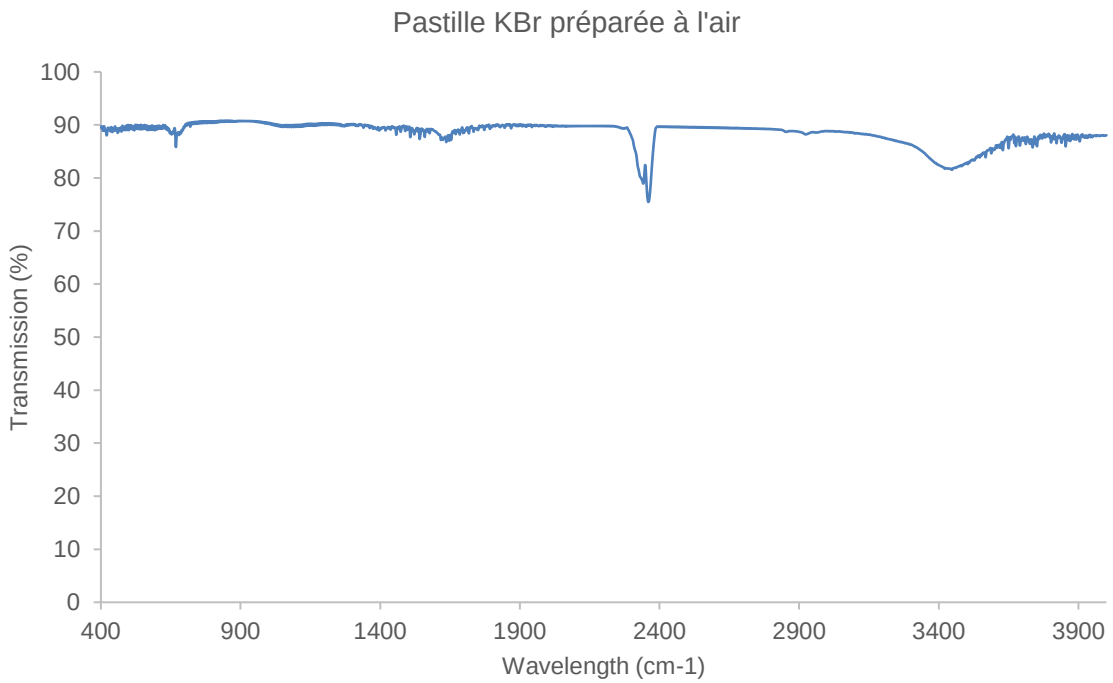

Source: Author's own

Unfortunately, the absorption under 1000cm-1 was too high because of the concentration of the solution, for a new measure a proportion of 0.5%wt is desirable. This region corresponds to the vibration bands for Al-O and could not be read in this analysis. The presence of water in all samples in this measure and not in the previous one shows that diluting the powder has a big impact on the results and measuring the samples without the solution gives better a measure, even though this will not impact on the readings around the Al-O peaks.

3.2.2 XPS of compressed samples

From the measurement of the mass before and after the analysis, only the humid samples showed a difference (Tab. 1). The water that escapes the sample because of the depressurizing is linked to the open porosity.

Table 1 - Mass difference before and after the XPS

Sample	Mass before (mg)	Mass after (mg)	Δmass (%)
Dry compacted sample	1.77	1.76	≈ 0
Humid compacted sample 1	0.94	0.83	11.70
Humid compacted sample 2	0.96	0.92	4.17

Source: Author's own

The specters reveal the presence of carbon, oxygen and aluminum. The carbon is a regular contaminant that was already expected because of the atmosphere and manipulation, especially because of the scotch tape used in the sample holder. Other contaminations were not found.

To evaluate stoichiometrically the O1s peak is the target to differentiate the presence of hydroxides and oxides, because the Al2p peak does not manifest a big change in terms of positioning[20]. In general, using XPS it can be quite difficult to find this difference and determine their presence. One method is to quantify the ration Al/O by observing the form of the O1s peak[21].

Since all specters are quite similar, the reproducibility of the samples and the analysis is quite good. The presence of a sharper edge at the base of the curve could be linked to lower binding energies which seems to correspond more to a differential charge effect than to a real chemical shift. When comparing the specters from the dry and humid powder, there is no enlargement that would necessarily mark the presence of the Al-O-H bond (Fig. 17).

[20] ZÄHR, J. *et al*, Characterisation of oxide and hydroxide layers on technical aluminum materials using XPS, **Vacuum**, v. 86, n. 9, p. 1216–1219, 2012.

[21] ALEXANDER, M R; THOMPSON, G E; BEAMSON, G, Characterization of the oxide/hydroxide surface of aluminium using x-ray photoelectron spectroscopy: a procedure for curve fitting the O 1s core level, **Surf. Interface Anal.**, p. 10, 2000.

Figure 17 - O1s peak of the three compacted samples (a)from the dry powder (b)and(c)form the humid poder

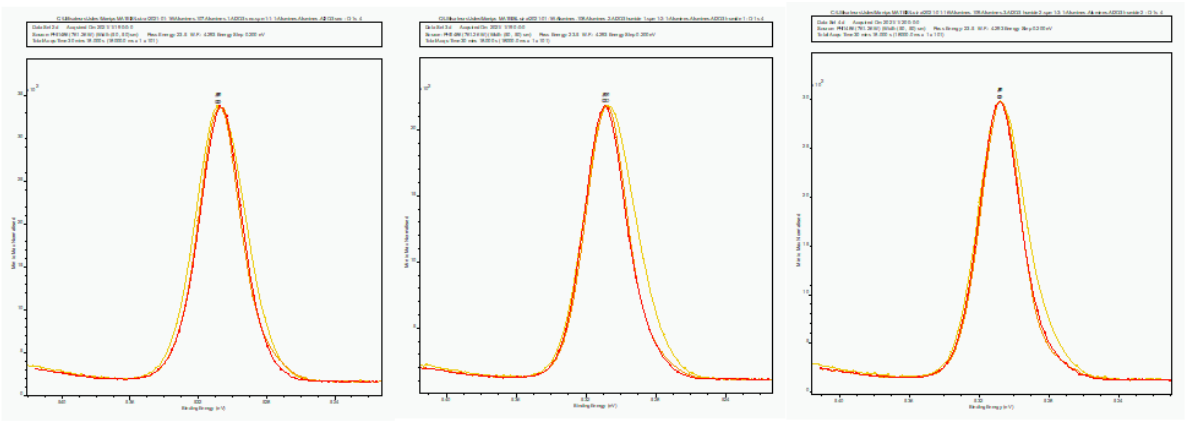

Source: Author's own

Knowing that there is a 1.4 eV energy gap between the Al-O-Al bond and the Al-O-H[22], a graph that shows the observed energy at the peaks in each of the three points in each sample is represented in Fig. 18. If there is a variation of the ration Al-O-H/Al-O-Al, that would implicate in a displacement of the curve at the center of the peak to the right. Each sample does not show a notable difference in this ratio. With this method it is possible to say that most of the atoms are linked as oxides and that the displacement could be linked to the presence of diaspore.

[22] ZÄHR *et al*, Characterisation of oxide and hydroxide layers on technical aluminum materials using XPS.

Figure 18 – Energy of the peaks

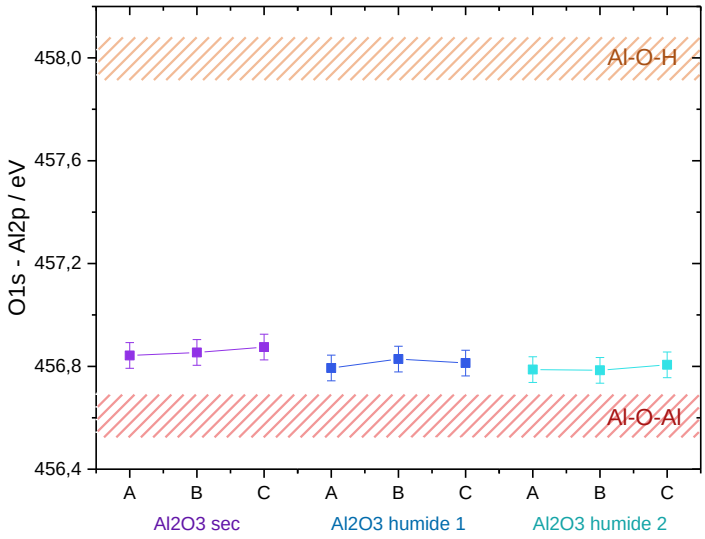

Source: Author's own

By integrating the values of the peaks for carbon, oxygen and aluminum, a quantification of the elements is possible. Fig. 19 shows the ration of Al/O, with a possible super estimation of the quantity of oxygen because, as seen in the FTIR, some of it is bonded to carbon. Annex B shows the obtained specters for the compact samples of the dry and humid powders for reference.

Figure 19 – Composition par element

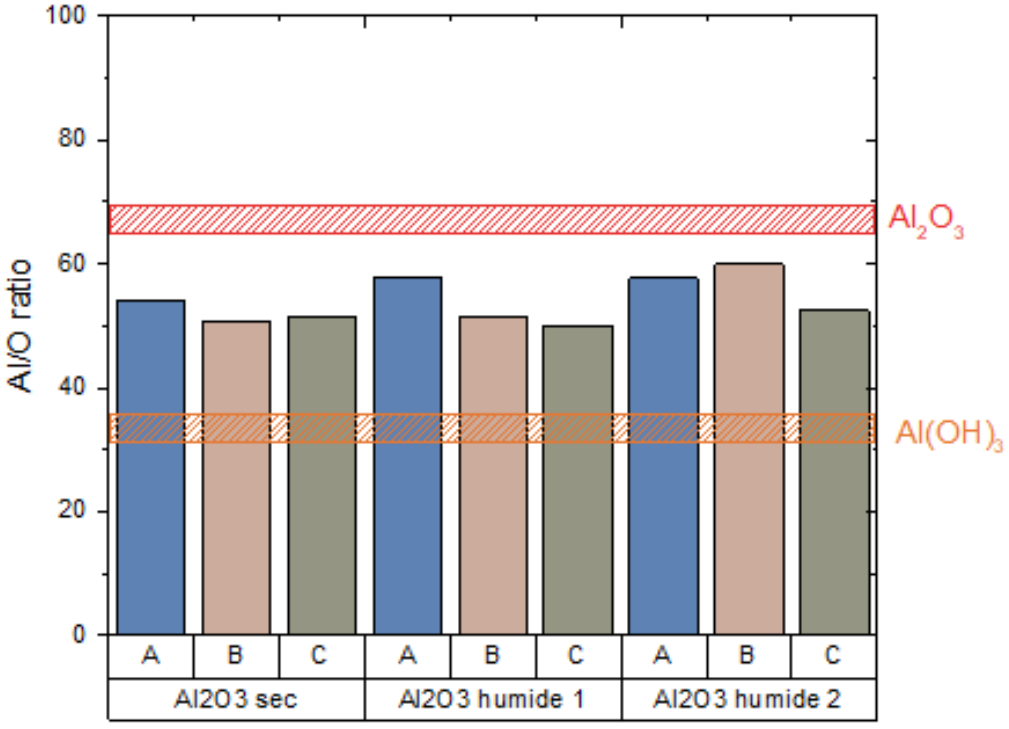

Source: Author's own

3.2.3 Accompanying the transformation of samples with DRX

The DRX analysis is used to determine which phases are present in the samples. Fig. 20 shows the specters obtained for both starting powders, the black curve corresponds to the dry one and the red is related to the humid. Their peaks are quite similar and can be identified as delta and gamma alumina, respectively the blue and the yellow in the image. There is one smaller peak that is only present in the humid powder around 40° but that is probably linked to a transition alumina phase.

Figure 20 – XRD for the powders

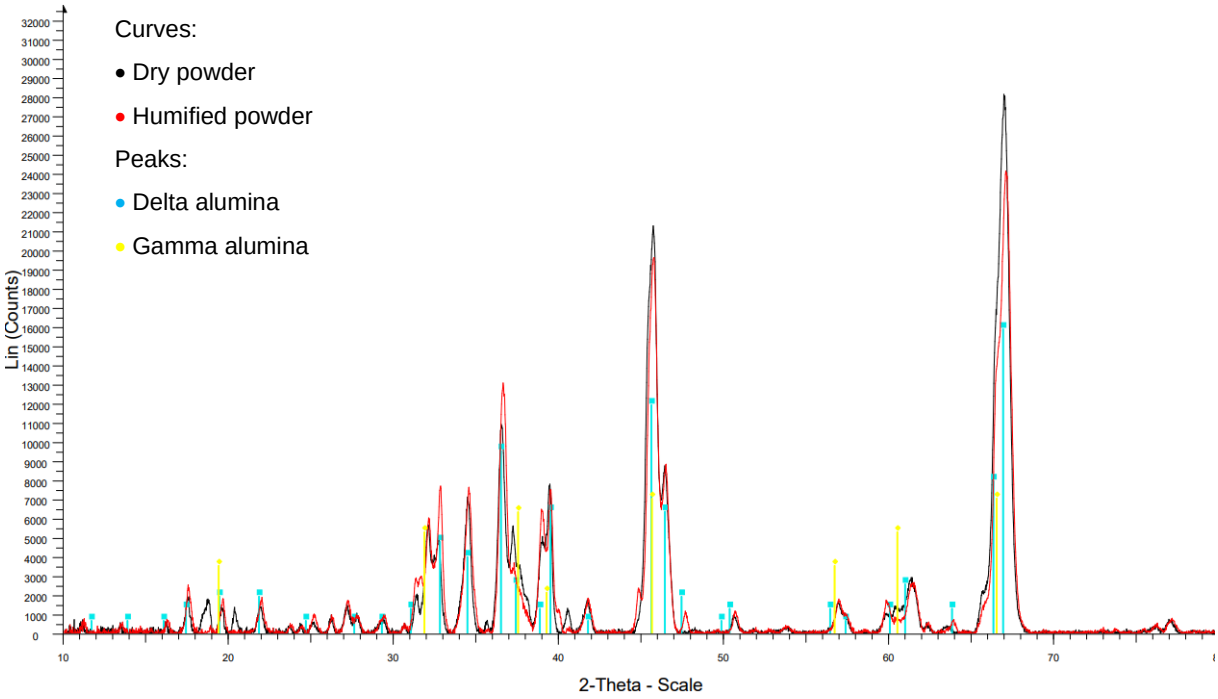

Source: Author's own

The same comparison was done between the compacted powders and is shown in Fig. 21. Both samples still have close specters, but the identifications of peaks are not as clear. Here the red curve refers to the humid compacted sample and the black one to the dry. Even though some peaks can be identified as delta, the region around 25-30° has unidentifiable peaks that cannot be found using the PDF Database from the EVA. These peaks are not present in the powder before compaction. Some peaks around 40° could reveal the presence of AlO although the sample did not go to high enough temperatures to transform in this specific oxide[23].

[23] HOCH, Michael; JOHNSTON, Herrick L., Formation, Stability and Crystal Structure of the Solid Aluminum Suboxides: Al_2O and AlO [1], **Journal of the American Chemical Society**, v. 76, n. 9, p. 2560–2561, 1954.

Figure 21 - XRD for the compacted samples

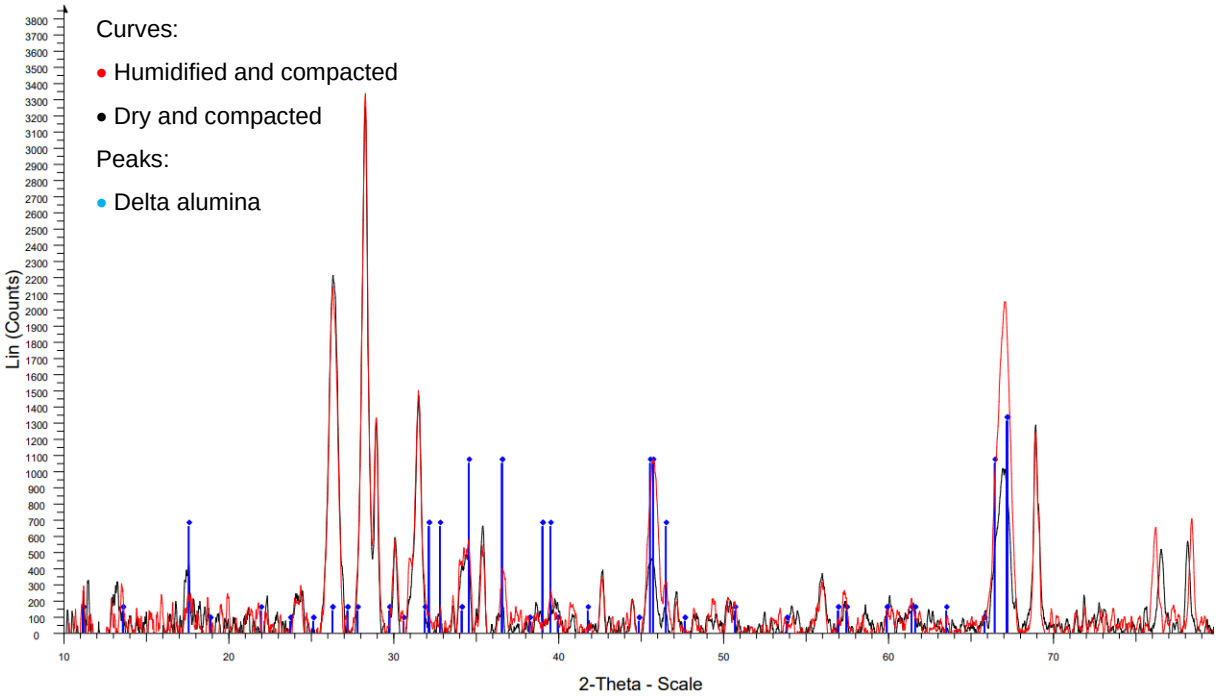

Source: Author's own

Figure 22 shows a comparation between the compacted and sintered samples with the black curve being from the dry powder and the blue from the humid using the peaks for corundum in red and for diaspore in green. The humid powder has more expressive peaks according to diaspore.

Figure 22 – XRD for the sintered samples

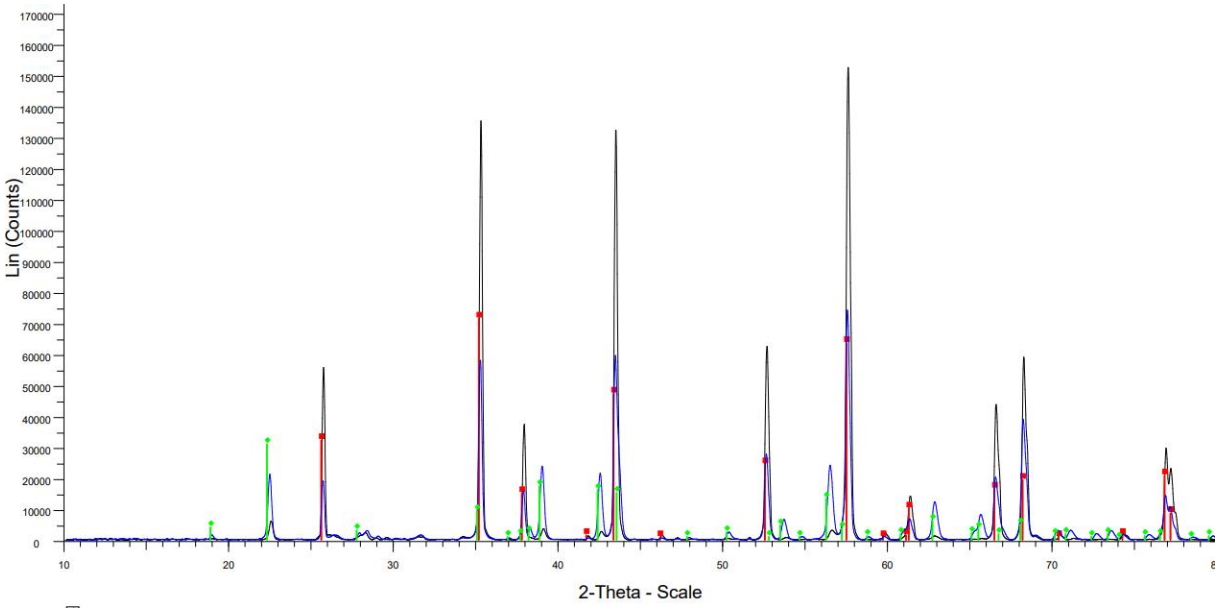

Source: Author's own

3.3 COMPOSITION

The refinement done for the powders is just an estimation, but for reference the table below shows the composition found. Both powders had close values (Tab. 2), this calculation was done using the specters shown in Annex C (a).

Table 2 – Composition of the powders

Phase	wt. %
Gamma	18
Theta	2
Delta	40
Delta*	40

Source: Author's own

The peaks for the compacted samples were not sufficient to make the same calculation according to the available database. There is a possibility that there is formation of AlO under high pressure, but further investigation is needed to attest whether it is possible on this samples.

The cylindric samples from the dry powder, compressed at 5GPa, that were sintered were also analyzed considering they had different aspects because one side had an important gold contamination and some peaks that could not be identified, possibly diaspore, quartz or even carbon, that gave a dark aspect to the surface, this composition is given on Tab. 3.

Table 3 – Composition of the compacted and sintered sample from the dry poder

Phase	wt. %
Corundum	97
Gold	3

Source: Author's own

The other side, with a whiter appearance, did not manifest the same contamination and had corundum mixed with some diaspore, as shown in Tab. 4.

Table 4 - Composition of the compacted and sintered sample from the dry powder

Phase	wt. %
Corundum	97
Diaspore	3

Source: Author's own

Another compacted sample from the dry powder, elaborated inside the pelletizer; this one had a little more diaspore, shown in Tab. 5.

Table 5 – Composition of the compacted and sintered sample from the dry powder

Phase	wt. %
Corundum	92
Diaspore	8

Source: Author's ownù

The compacted sample from the humid powder had a more unique composition, since the presence of diaspore was much more significative, which was to be expected from the sintered specters (Fig. 22).

Table 6 – Composition of the compacted and sintered sample from the humid powder

Phase	wt. %
Corundum	53
Diaspore	47

Source: Author's own

3.4 NANOCOMPRESSION

The nano compression was supposed to be performed in thin layers obtained from the compacted samples for both powders but for the humid one it did not work because the indentation could not be done on the sample. Fig. 23 shows the exploitation of the of the images obtained from the microscope as to measure the displacement camp. The value at the right corner of the image corresponds to the

equivalent displacement, which is always a positive value. The deformation is really localized which makes it harder to precisely make the calculation of deformation in spots farther from the indent. The problem with the resulting image is that it is not capable to capture the fissure right under the indent.

Figure 23 – Nanocompression of the dry compacted sample

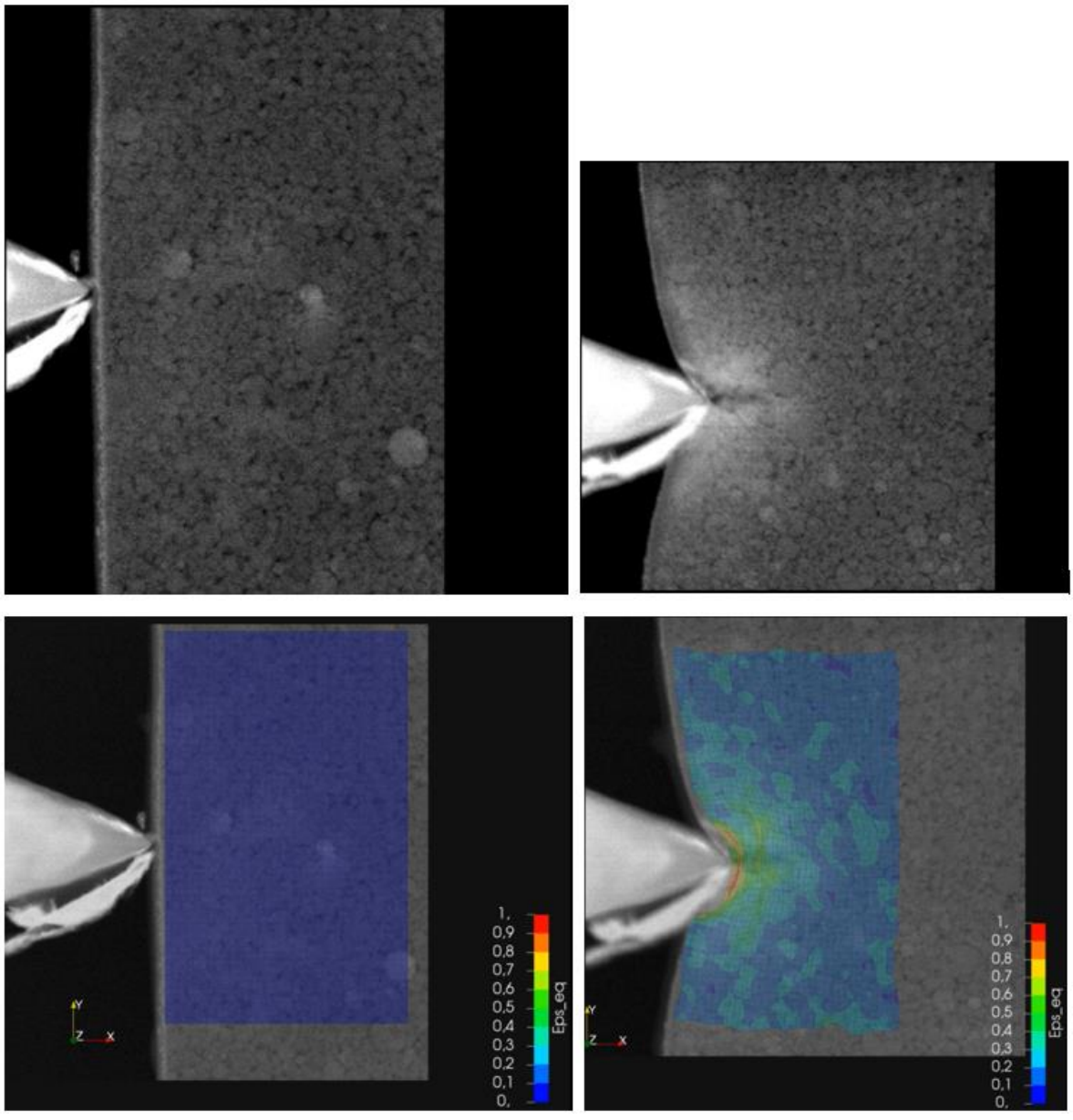

Source:

4 DISCUSSION

From the initial three characterization methods, none could differentiate each powder. Contrary to the initial assumptions, in the primary states of the powder, having water or not does not impact in the structure of the alumina, since, as seen in XRD and X-Ray diffraction, both samples had similar specters. Although there is a clearer presence of diaspore for the sintered and compacted sample of humid powder.

Diaspore can be an alteration of corundum [24] that is caused by the presence of water in the powder since the other one turned mostly to alpha. In Fig. 4, different minerals can originate alpha alumina according to their hidratation and sintering temperatures. The sintering used in this study is rather low when compared to most transformations shown in the image. For the dry powder, alpha alumina was already obtained at 560°C, low when compared to the 1200°C from Silva (2016). At the same time its observation is linked to the calcination of minerais found in bauxite, unlike the nanometric alumina studied.

Figure 24 - Alumine transformations

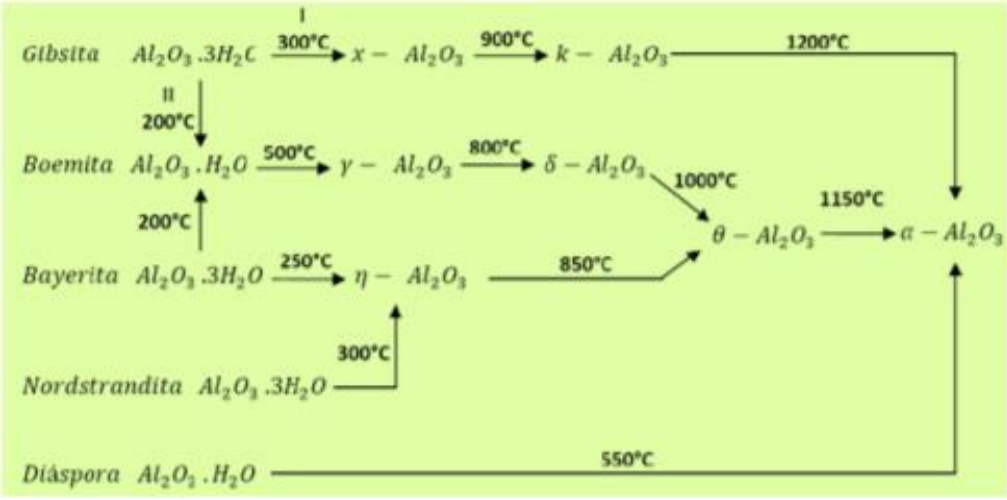

Source: SILVA, F M N; LIMA, E G; RODRIGUES, M G F, INFLUÊNCIA DA CALCINAÇÃO NAS TRANSFORMAÇÕES DE FASE DA GIBSITA-BOEMITA-GAMA/ALUMINA, p. 11, 2016.

The transformation involved for this study implies that delta and gamma alumine from a nanometric powder can turn into alpha with low temperatures. Additionally, humidifying the powder before processing alters the transformation. Instead of going

[24] **Hydroxides | Elsevier Enhanced Reader**, disponível em: <https://reader.elsevier.com/reader/sd/pii/B9780081029084001624?token=784FB4230544B76ADCAFB7B53835716F68FBF85563A0EE00255FB420985109723D738EE39717A7F3DCDB0E5506A58740&originRegion=us-east-1&originCreation=20211104002625>. acesso em: 3 nov. 2021.

directly from gamma and delta to alpha, it has an additional step becoming diaspore with sintering around 500°C.

5 CONCLUSIONS

The treatment of the powders does have an impact on the compression and sintering of samples. The XRD analysis revealed that hydrating the powder generates a greater percentage of diaspore than using a dry powder. Meanwhile, when analyzing the compacted samples, there is no notable difference between the samples when measuring them with the XRD or the FTIR.

The XPS does not give information about the phases but could have been used to study the inside of the sample to have a more complete overview of the differences between the surface and the bulk, even though this manipulation can be difficult as to avoid the effects of the atmosphere.

Nano compression proved there is a great difference in behavior between the two compacted samples, because the thin layer obtained from the humid sample did not stand the indentation because of a lack of consistency between particles at this level.

REFERÊNCIAS

1. ASSOCIAÇÃO BRASILEIRA DE NORMAS TÉCNICAS. **NBR 14724:** Informação e documentação — Trabalhos acadêmicos — Apresentação. Rio de Janeiro: 2011. 11 p.
2. DIVISÃO DE BIBLIOTECA, ESCOLA POLITÉCNICA DA UNIVERSIDADE DE SÃO PAULO. **Diretrizes Para Apresentação de Dissertações e Teses**. 4ª. ed. São Paulo: 2013. 95 p.
3. ASSOCIAÇÃO BRASILEIRA DE NORMAS TÉCNICAS. **NBR 6023:** Informação e documentação - Referências - Elaboração. Rio de Janeiro: 2002. 24 p.

APPENDIX A

Raw results from the FTIR performed on the powders and on compacted samples

FTIR of both powders at a starting state and after compaction with some identified peaks

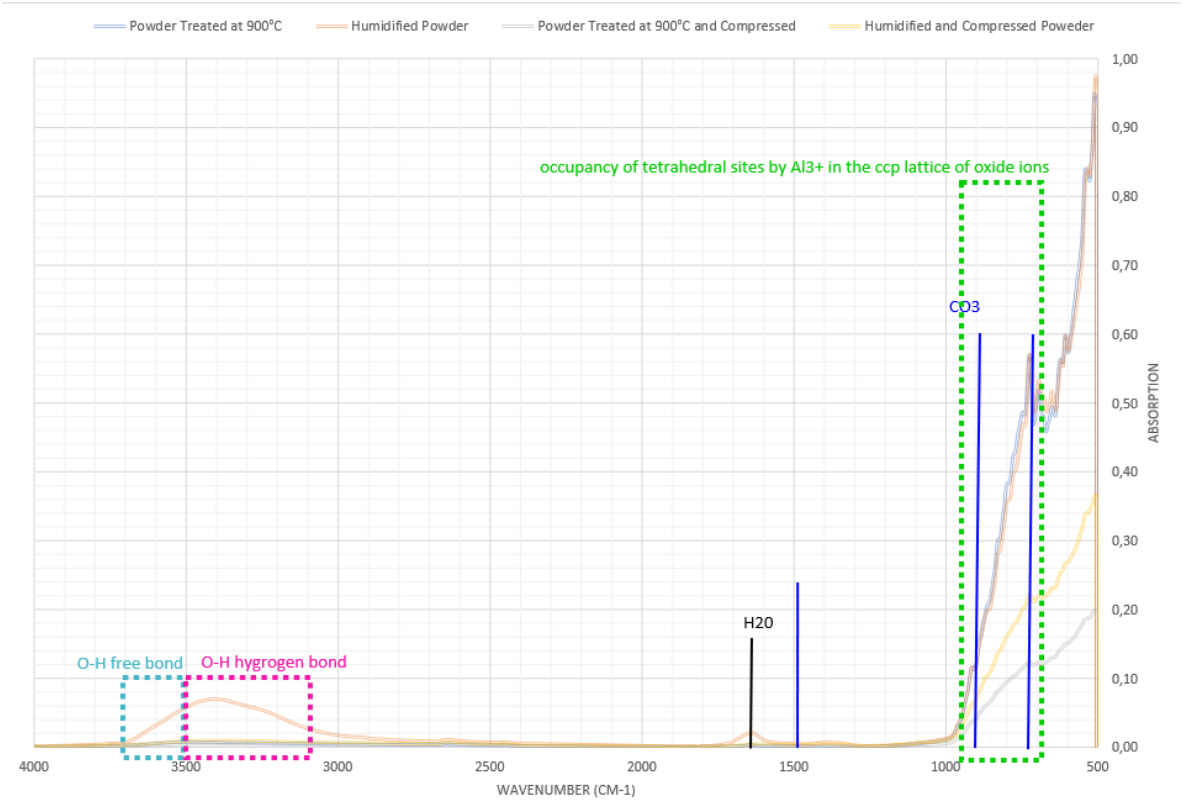

APPENDIX B

Raw XPS from the three compacted samples done on Sureval

Compacted sample from the dry powder

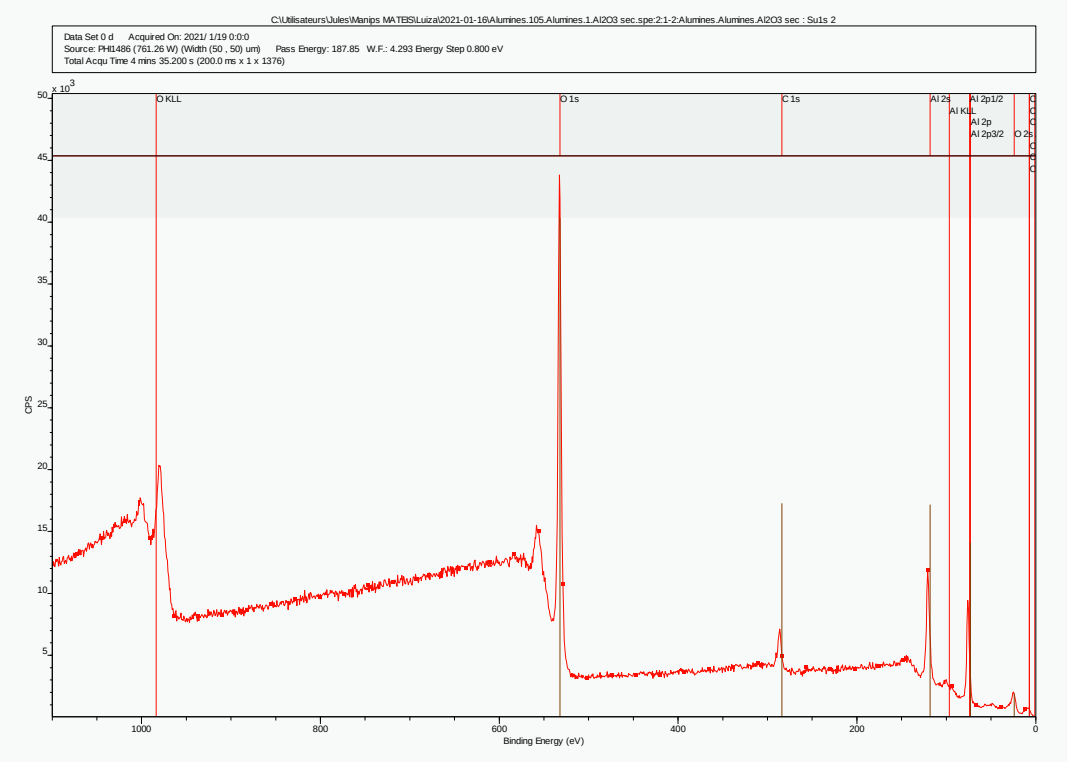

Compacted sample from the humid powder

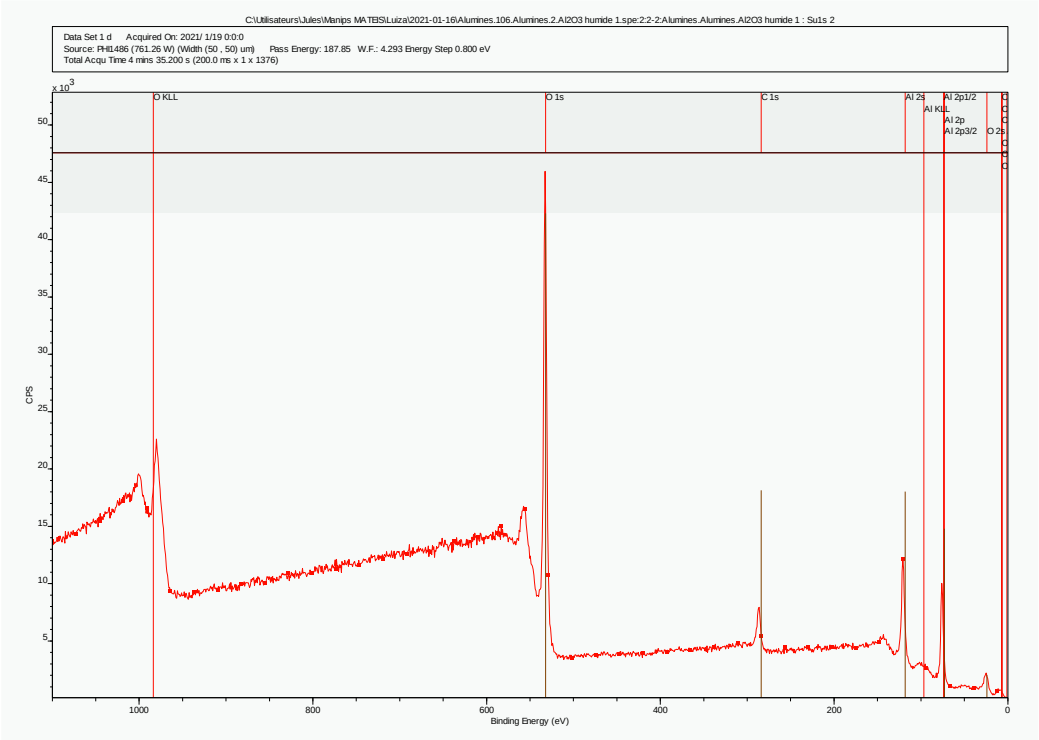

APPENDIX C

Raw XRDs from the starting powders and their compacted samples

Dry powder with gamma (yellow) and delta (blue) peaks identified

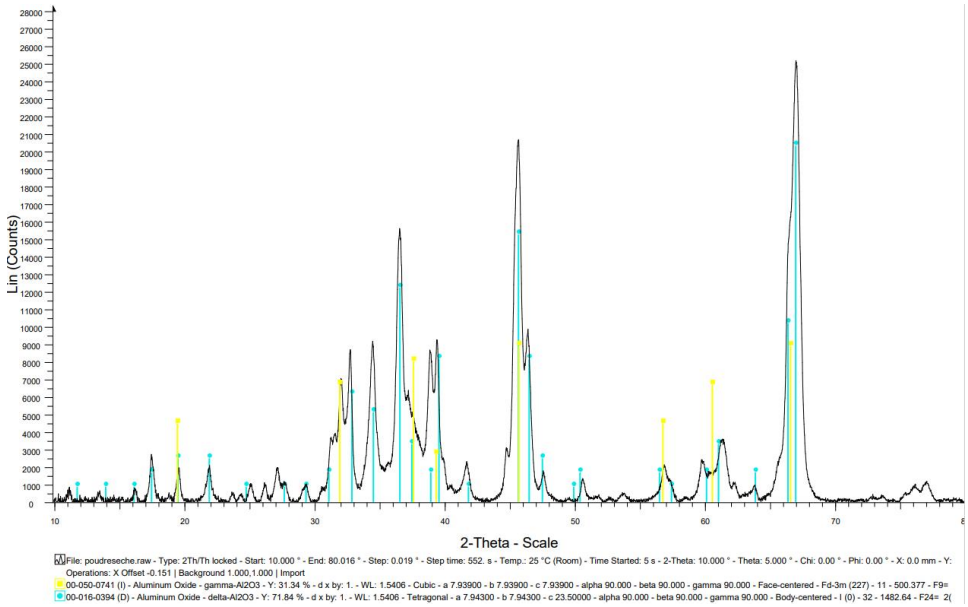

Humid powder with gamma (yellow) and delta (blue) peaks identified

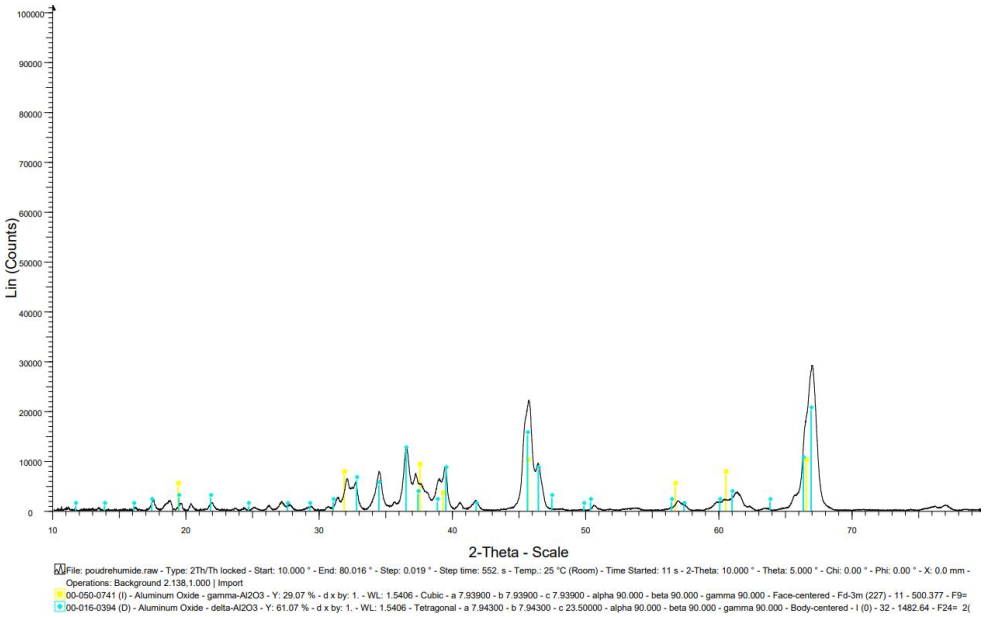

Compacted sample from the humid powder with delta (blue) and gamma (yellow) peaks identified

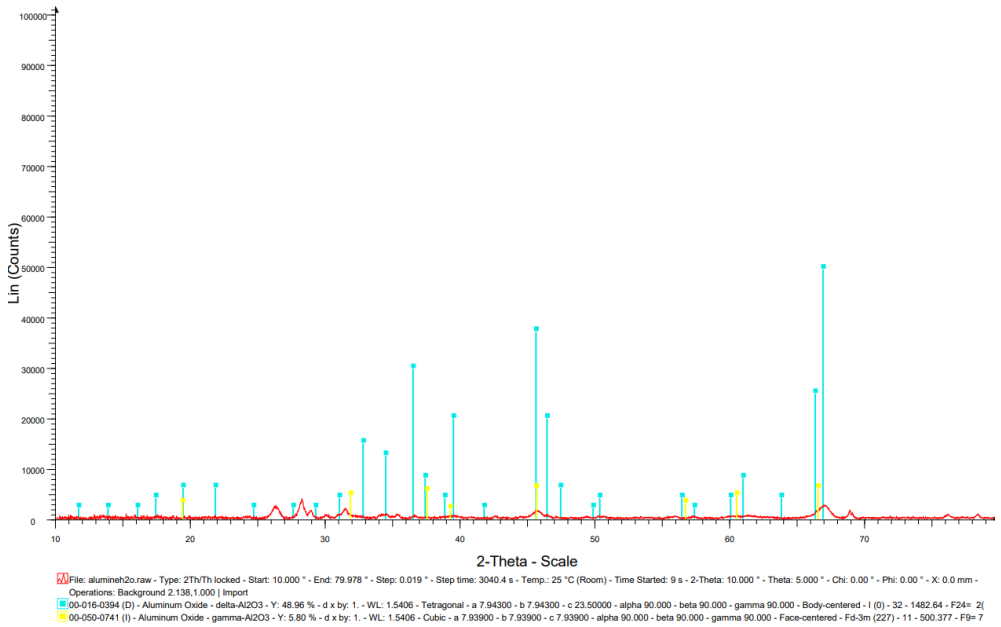

Comparation between dry powder (red), and its compacted (green) and sintered (black) samples with alpha (red) and delta (blue) peaks identified

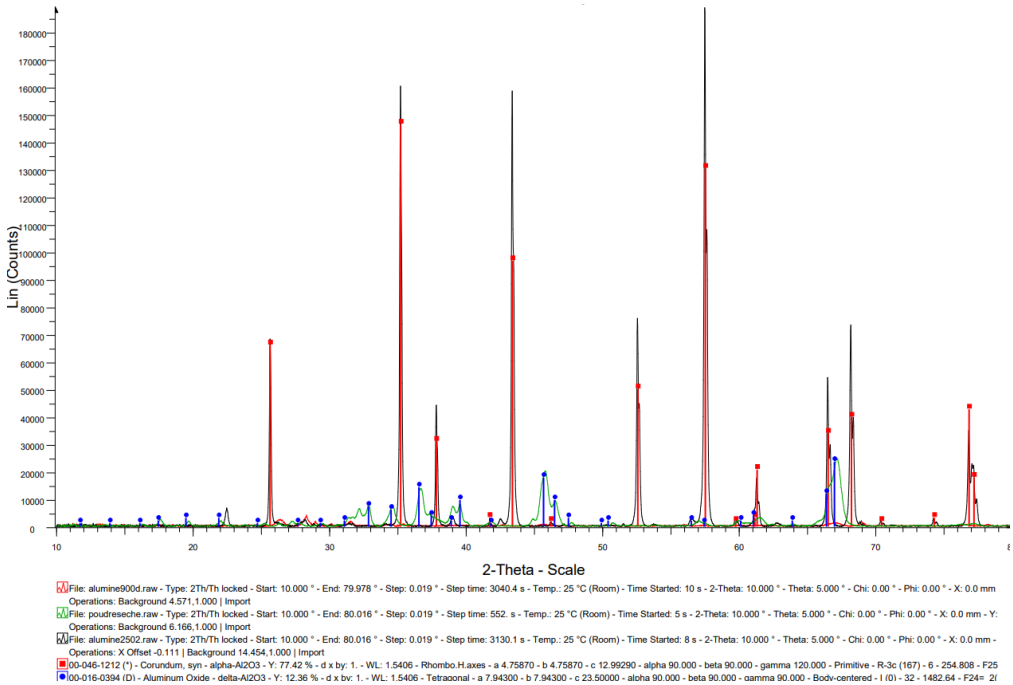

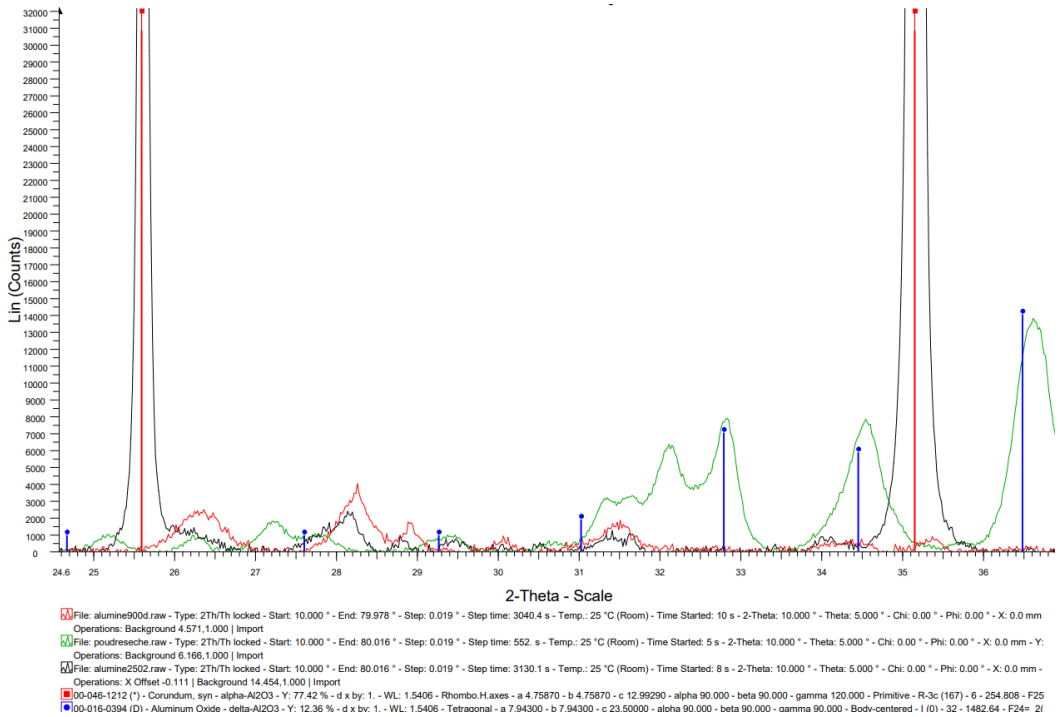

Comparation between humid powder (blue), and its compacted (red) and sintered (black) samples with alpha (red) and diaspore (green) peaks identified